

CircRNA expression profiles in human visceral preadipocytes and adipocytes

WENXING SUN¹, XUECHENG SUN², WEIWEI CHU³, SHIGANG YU⁴, FULU DONG⁵ and GUANGFEI XU¹

¹Department of Nutrition and Food Hygiene, School of Public Health, Nantong University, Nantong, Jiangsu 226019;

²Department of Trauma Surgery, Weifang People's Hospital, Weifang, Shandong 26100; ³School of Pharmaceutical Sciences (Shenzhen), Sun Yat-sen University, Guangzhou, Guangdong 510275; ⁴Engineering Research Center of Sichuan Province Higher School of Local Chicken Breeds Industrialization in Southern Sichuan, College of Life Science, Leshan Normal University, Leshan, Sichuan 614000; ⁵Laboratory of Nuclear Receptors and Cancer Research, Center for Basic Medical Research, Medical College, Nantong University, Nantong, Jiangsu 226019, P.R. China

Received June 24, 2019; Accepted November 8, 2019

DOI: 10.3892/mmr.2019.10886

Abstract. Circular RNAs (circRNAs) regulate several physiological and pathological processes, but their role in visceral lipid deposition has not been explored. In the present study, human preadipocytes from visceral fat tissue (HPA-v) were induced to form adipocytes, and the circRNA expression profiles in HPA-v and adipocytes were detected using circRNA microarrays. The microarray data revealed that 2,215 and 1,865 circRNAs were significantly up- and down-regulated, respectively, in adipocytes compared with HPA-v. Moreover, the parental genes of differentially expressed circRNAs were associated with fatty acid metabolism based on Kyoto Encyclopedia of Genes and Genomes analysis. Three circRNAs (hsa_circ_0136134, hsa_circ_0017650, and hsa_circRNA9227-1) were selected for quantitative PCR (qPCR) validation, and the qPCR results were consistent with the microarray results. Furthermore, MiRanda software was used to predict the microRNAs (miRNAs) potentially targeting the top 10 up- and downregulated circRNAs, and 14 miRNAs with more than two miRNA response elements targeting these circRNAs. This is the first study of the expression profiles of circRNAs in HPA-v and adipocytes and may suggest potential therapeutic targets for the visceral obesity.

Introduction

Obesity, especially excess visceral lipid deposition, increases the risks of numerous diseases, including type 2 diabetes, cardiovascular disease, and some cancers (1-4). Generally, obesity involves hypertrophy and hyperplasia of excess adipocytes (5,6). Adipocyte hyperplasia is dependent on preadipocyte proliferation and differentiation. Research on adipocyte hyperplasia has been focused largely on deciphering the molecular mechanisms underlying obesity and developing novel therapeutics for obesity.

Circular RNAs (circRNAs) are non-coding RNAs that form a closed circular loop by back-splicing circularization (7), and they exhibit higher stability and resistance against RNA exonucleases compared with linear RNAs (8). Recent research has revealed that circRNAs regulate gene expression via multiple mechanisms, such as regulating gene transcription and splicing (9,10), acting as microRNA (miRNA) sponges (11), and forming RNA-protein complexes (12). Moreover, some circRNAs can be transcribed into proteins (13). In mammals, circRNA expression is tissue- and developmental stage-specific (14). Numerous studies have reported that circRNAs participate in the regulation of various physiological and pathological processes, such as regulating myogenesis and tumorigenesis (13,15,16). However, the role of circRNAs in visceral adipogenesis has not been investigated, and no circRNA examined to date has been associated with visceral adipogenesis.

Examination of the genes differentially expressed in preadipocytes and adipocytes should identify novel factors promoting or inhibiting lipid deposition. To identify the circRNAs associated with visceral adipocyte hyperplasia, the expression profiles of circRNAs in human preadipocytes derived from visceral fat tissue (HPA-v) and adipocytes were analyzed using circRNA microarrays. The results revealed that HPA-v and visceral adipocytes had different circRNA expression patterns, and the parental genes of the differentially expressed circRNAs were related to lipid metabolism; moreover, the candidate circRNAs were revealed to target many potential miRNA sites.

Correspondence to: Dr Fulu Dong, Laboratory of Nuclear Receptors and Cancer Research, Center for Basic Medical Research, Medical College, Nantong University, 19 Qixiu Road, Nantong, Jiangsu 226019, P.R. China
E-mail: fldste@163.com

Dr Guangfei Xu, Department of Nutrition and Food Hygiene, School of Public Health, Nantong University, 9 Seyuan Road, Nantong, Jiangsu 226019, P.R. China
E-mail: gfxu001@aliyun.com

Key words: microarray, circular RNAs, visceral preadipocytes, adipocytes

Materials and methods

Preadipocyte differentiation. HPA-v (cat. no. 7210; ScienCell Research Laboratories, Inc.) were isolated from human visceral fat tissue and cultured in preadipocyte medium (cat. no. 7211; ScienCell Research Laboratories, Inc.) containing 5% fetal bovine serum, 100 IU/ml penicillin-streptomycin, and 1% preadipocyte growth supplement (cat. no. 7252; ScienCell Research Laboratories, Inc.). After reaching confluence, the HPA-v were induced to differentiate for 3 days in DMEM containing 0.1 mM 3-isobutyl-1-methylxanthine, 1 μ M dexamethasone, and 5 μ g/ml insulin. The differentiated HPA-v were then maintained in DMEM containing 5 μ g/ml insulin for 6 days.

Oil Red O staining. Cellular lipids were detected using Oil Red O staining. Briefly, upon reaching 100% confluence or differentiation, the preadipocytes were washed three times with phosphate-buffered saline and fixed in 10% formalin for 15 min at room temperature. After fixation, the cells were stained with Oil Red O for 20 min at room temperature. Stained cells were visualized using a Leica DMI 4000 B fluorescent microscope on the white light setting (magnification, x100).

Total RNA isolation. Total RNA was isolated from 5x10⁶ HPA-v cells and adipocytes, which were differentiated from HPA-v cells, using TRIzol[®] reagent (cat. no. 15596018; Invitrogen; Thermo Fisher Scientific, Inc.) and reverse transcribed into cDNA using the HiScript III 1st Strand cDNA Synthesis kit (cat. no. R312-01; Vazyme Biotech Co., Ltd.), according to the manufacturer's protocol. RNA integrity was evaluated by electrophoresis on 2% (w/v) denaturing agarose gels. The concentration and purity of RNA were determined according to the OD₂₆₀/OD₂₈₀ values using the NanoDrop1000 Spectrophotometer (Thermo Fisher Scientific, Inc.).

CircRNA microarray analysis. A human circRNA microarray (Agilent Technologies, Inc.) containing 170,340 human circRNA probes was used. Six samples (three HPA-v and three adipocyte samples) were detected by CapitalBio Corporation using circRNA microarrays. CircRNAs were purified, amplified, labeled with Cy3-dCTP, and hybridized onto the circRNA array according to the manufacturer's protocol. The circRNA expression data were normalized using the GeneSpring GX software version 13.0 (<https://www.agilent.com>). Differentially expressed circRNAs between HPA-v and adipocytes were selected according to the following thresholds: |fold change| ≥ 5 and P-value < 0.01. Volcano plots were generated to visualize the circRNAs differentially expressed between HPA-v and adipocytes. Hierarchical cluster analysis was used to evaluate differential circRNA expression patterns across the six samples. The parental genes of the differentially expressed circRNAs were analyzed using the Kyoto Encyclopedia of Genes and Genomes (KEGG) database within the Database for Annotation, Visualization and Integrated Discovery (<https://david.ncifcrf.gov>). The homology of circRNAs between human and mice was analyzed using CIRCpedia version 2 software (<http://circatlas.biols.ac.cn>). The miRNA response elements (MERs) within circRNAs were predicted using MiRanda version 3.3 software (<http://www.microrna.org>).

Quantitative PCR (qPCR). The expression levels of peroxisome proliferator-activated receptor gamma 2 (*PPARG2*), CCAAT enhancer binding protein alpha (*CEBPA*), fatty acid binding protein 4 (*FABP4*), hsa_circ_0136134, hsa_circ_0017650, and hsa_circRNA9227-1 were detected by qPCR. Ribosomal protein lateral stalk subunit P0 (*RPLP0*) was used as an invariant control. qPCR was performed using the ChamQ SYBR[®] qPCR Master mix (cat. no. Q311-02; Vazyme Biotech Co., Ltd.), according to the manufacturer's instructions, on an ABI 7300 instrument (ABI; Thermo Fisher Scientific, Inc.). The primers used for qPCR were as follows: *PPARG2* forward, 5'-CGGATTGATCTTTTGCTA-3' and reverse, 5'-CTTTCTGGGTCAATAGGAG-3'; *CEBPA* forward, 5'-CGTGGAGACGCAGCAGAA-3' and reverse, 5'-GGCCTTGACCAAGGAGCT-3'; *FABP4* forward, 5'-CAG CACCCTCTGAAAAC-3' and reverse, 5'-GCAAAGCCC ACTCCTACT-3'; *RPLP0* forward, 5'-CTCTGCATTCTC GCTTCC-3' and reverse, 5'-GACTCGTTTGTACCCGTT G-3'; hsa_circ_0136134 forward, 5'-AAGGCACCTGCGGTA TTT-3' and reverse, 5'-AGCCACGGACTCTGCTACT-3'; hsa_circ_0017650 forward, 5'-AAGACCTTCCTCCTTTAC CC-3' and reverse, 5'-GCAACAGTCTGACTTGCCCTC-3'; and hsa_circRNA9227-1 forward, 5'-CCGACGCACCATCAG TTT-3' and reverse, 5'-GAGCGAGGCACAGAAAGG-3'. The thermocycling conditions for the qPCR were as follows: Initial denaturation at 95°C for 30 sec; 45 cycles of denaturation at 95°C for 5 sec; and annealing and extension at 60°C for 30 sec. The relative expression levels of RNA were analyzed with the 2^{- $\Delta\Delta C_q$} method (17) and normalized to the loading control RPLP0.

Statistical analysis. The data are presented as the means \pm standard deviation. The significance of the differences was analyzed using Student's t-test. P < 0.05 was considered to indicate a statistically significant difference.

Results

HPA-v differentiation. To obtain mature visceral adipocytes, HPA-v were induced to differentiate in medium containing 0.1 mM 3-isobutyl-1-methylxanthine, 1 μ M dexamethasone, and 5 μ g/ml insulin. The characteristics of HPA-v differentiation were confirmed by Oil Red O staining and evaluation of adipogenic marker gene expression (Fig. 1). Oil Red O staining revealed substantial lipid deposition in the cytoplasm after differentiation (Fig. 1A). In addition, *PPARG2*, *CEBPA* and *FABP4* mRNA expression levels were significantly increased in mature visceral adipocytes (Fig. 1B).

Expression profiles of circRNAs in HPA-v and adipocytes. To investigate whether circRNAs are associated with lipid deposition, a human circRNA microarray (version 2.0; Agilent Technologies, Inc.) was used to assess circRNA expression profiles in HPA-v and adipocytes. The distribution of circRNA expression was illustrated in a box plot after normalization using the GeneSpring GX software (Fig. 2A), which revealed that the distribution of log₂ ratios was similar among all samples. Volcano plots were generated to compare the circRNA expression profiles between HPA-v and adipocytes (Fig. 2B). The circRNAs differentially expressed between HPA-v and

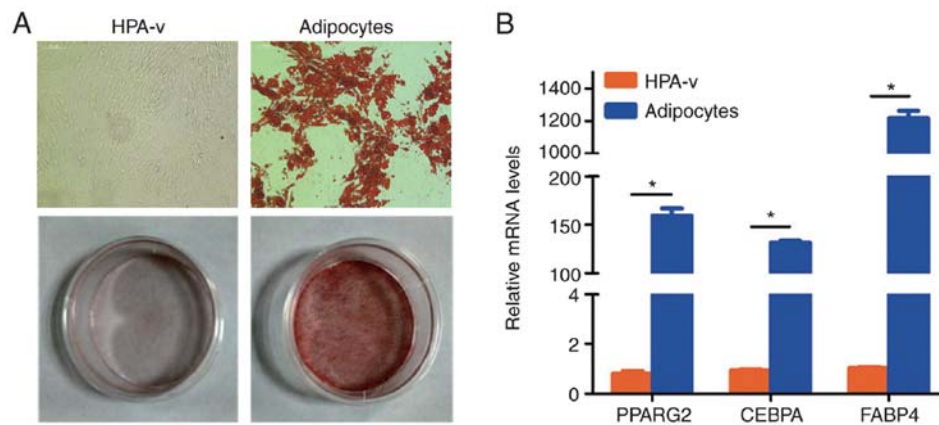


Figure 1. Characteristics of differentiated HPA-v. (A) Lipid droplets were detected by Oil Red O staining in HPA-v and adipocytes (magnification, x100). (B) The expression of adipogenic marker genes in HPA-v and adipocytes was analyzed by qPCR. * $P < 0.05$. HPA-v, human preadipocytes from visceral fat tissue; *PPARG2*, peroxisome proliferator-activated receptor gamma 2; *CEBPA*, CCAAT enhancer binding protein alpha; *FABP4*, fatty acid binding protein 4.

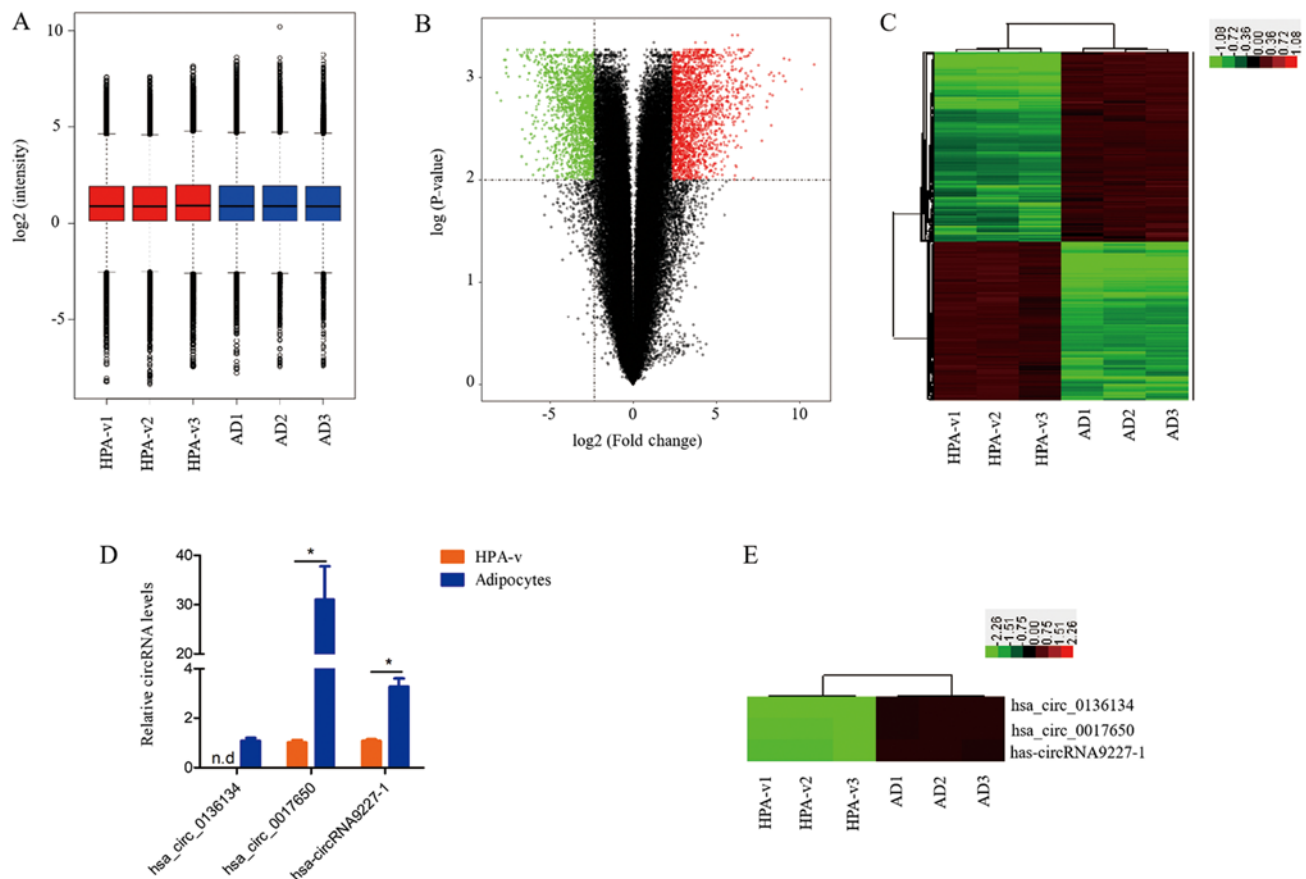


Figure 2. Comparison of circRNA expression profiles between HPA-v and adipocytes. (A) Box plots revealed the distribution of circRNAs in the six samples after normalization. (B) Volcano plots revealed the differentially expressed circRNAs. Green and red dots represent significantly down- and upregulated circRNAs in adipocytes compared with HPA-v, respectively (fold change ≥ 5.0 , $P < 0.01$). (C) Hierarchical clustering was performed to reveal the differentially expressed circRNAs between HPA-v and adipocytes. (D) Expression patterns of select differentially expressed circRNAs in HPA-v and adipocytes were determined by qPCR. (E) The heatmap revealed the selected differentially expressed circRNAs in HPA-v and adipocytes. * $P < 0.05$. circRNA, circular RNA; HPA-v, human preadipocytes from visceral fat tissue; AD, adipocytes; n.d., not detected.

adipocytes were identified as those with a fold change ≥ 5.0 and a P -value ≤ 0.01 . In total, 2,215 up- and 1,865 downregulated circRNAs were identified in adipocytes compared with HPA-v (Table S1). Table I lists the top 10 up- and downregulated circRNAs, and the homologous circRNAs of hsa_circ_0094183, hsa_circ_0116913 in mice were MMU_CIRCpedia_216382,

MMU_CIRCpedia_14213, respectively, while the other 18 circRNAs did not find their homologous circRNAs in mice (Table I). The expression patterns of the differentially expressed circRNAs were visualized by hierarchical cluster analysis (Fig. 2C), which indicated different expression circRNA patterns between visceral adipocytes and HPA-v.

Table I. Top 10 up- and downregulated circRNAs in adipocytes.

circRNA ID	Fold change	Regulation	Conservation
hsa_circ_0136134	1925.3240	Up	Species-specific
hsa_circ_0136132	1141.0890	Up	Species-specific
hsa_circ_0136131	680.3070	Up	Species-specific
hsa_circ_0067409	581.1932	Up	Species-specific
hsa_circ_0094183	546.6634	Up	MMU_CIRCpedia_216382
hsa_circ_0060972	526.6423	Up	Species-specific
hsa_circ_0017650	447.0942	Up	Species-specific
hsa_circ_0128428	355.4433	Up	Species-specific
hsa-circRNA9227-1	343.7039	Up	Species-specific
hsa_circ_0060971	336.8149	Up	Species-specific
hsa-circRNA9333-2	292.9276	Down	Species-specific
hsa-circRNA1786-2	248.5333	Down	Species-specific
hsa_circ_0116913	214.6204	Down	MMU_CIRCpedia_14213
hsa_circ_0023242	207.2891	Down	Species-specific
hsa_circ_0032023	197.7922	Down	Species-specific
hsa-circRNA9333-9	197.0217	Down	Species-specific
hsa-circRNA2910-9	187.1047	Down	Species-specific
hsa_circ_0032024	184.9652	Down	Species-specific
hsa_circ_0052586	125.1419	Down	Species-specific
hsa_circ_0003543	113.2247	Down	Species-specific

circRNAs, circular RNAs.

To examine the reliability of the circRNA microarray data, three circRNAs were selected for validation by qPCR. According to the qPCR results, hsa_circ_0136134 was detected in adipocytes exclusively, hsa_circ_0017650 and hsa-circRNA9227-1 were upregulated 30.0- and 2.3-fold in adipocytes compared with HPA-v, respectively (Fig. 2D). The qPCR results were consistent with those of the circRNA microarrays (Fig. 2D and E).

General characteristics of the differentially expressed circRNAs. The distribution of the differentially expressed circRNAs on human chromosomes was analyzed, and the that 4,080 differentially expressed circRNAs were derived from genes located on all chromosomes, although rarely on chromosomes 13, 18, 21, and Y (Fig. 3A). When the distribution of these circRNAs was analyzed among the parental genes, it was revealed that 3,968 (97.25%) circRNAs were mapped to 971 parental genes, with 437 (45.01%) parental genes generating one circRNA and 179 (18.43%) parental genes generating more than five circRNAs (Fig. 3B).

KEGG analysis of the circRNA parental genes. To investigate the potential functions of the differentially expressed circRNAs, 971 parental genes were analyzed using the KEGG database. The top 15 most significantly enriched pathways, which included fatty acid metabolism, fatty acid degradation, fatty acid biosynthesis, and PPAR signaling pathways are presented in Fig. 4. The most significantly enriched pathway was fatty acid metabolism ($P=7.83E-08$), and most genes were involved in metabolic pathways (Gene count=104).

Table II. miRNAs with >2 miRNA response elements targeting the top 10 upregulated and downregulated circRNAs.

miRNA ID	circRNA ID
hsa-miR-3138	hsa_circ_0136134
hsa-miR-4717-5p	hsa_circ_0067409
hsa-miR-665	hsa-circRNA9227-1
hsa-miR-6791-5p	hsa_circ_0060971
hsa-miR-4725-3p	hsa-circRNA9333-2
hsa-miR-6824-5p	hsa-circRNA9333-2
hsa-miR-6808-5p	hsa-circRNA2910-9
hsa-miR-4514	hsa-circRNA2910-9
hsa-miR-6752-5p	hsa-circRNA2910-9
hsa-miR-6757-5p	hsa-circRNA2910-9
hsa-miR-7112-5p	hsa-circRNA2910-9
hsa-let-7e-5p	hsa_circ_0052586
hsa-miR-6840-3p	hsa_circ_0052586
hsa-miR-7851-3p	hsa_circ_0052586

circRNAs, circular RNAs; miRNA/miR, microRNA.

CircRNA-miRNA interactions. To dissect the potential functions of differentially expressed circRNAs, the MERs of top 10 up- and downregulated circRNAs were predicted. Table II lists the miRNAs with more than two MERs targeting the top 10 up- and downregulated circRNAs.

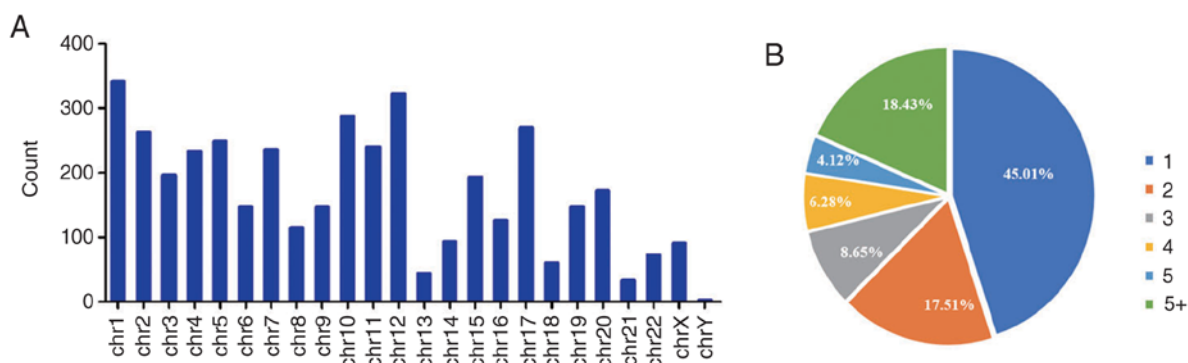


Figure 3. General characteristics of the differentially expressed circRNAs. (A) Chromosome distributions of the 4,080 circRNAs. (B) The percentages of six types of circRNAs, 1, 2, 3, 4, 5 and 5+ denote the number of differentially expressed circRNAs in the parental gene. circRNAs, circular RNAs.

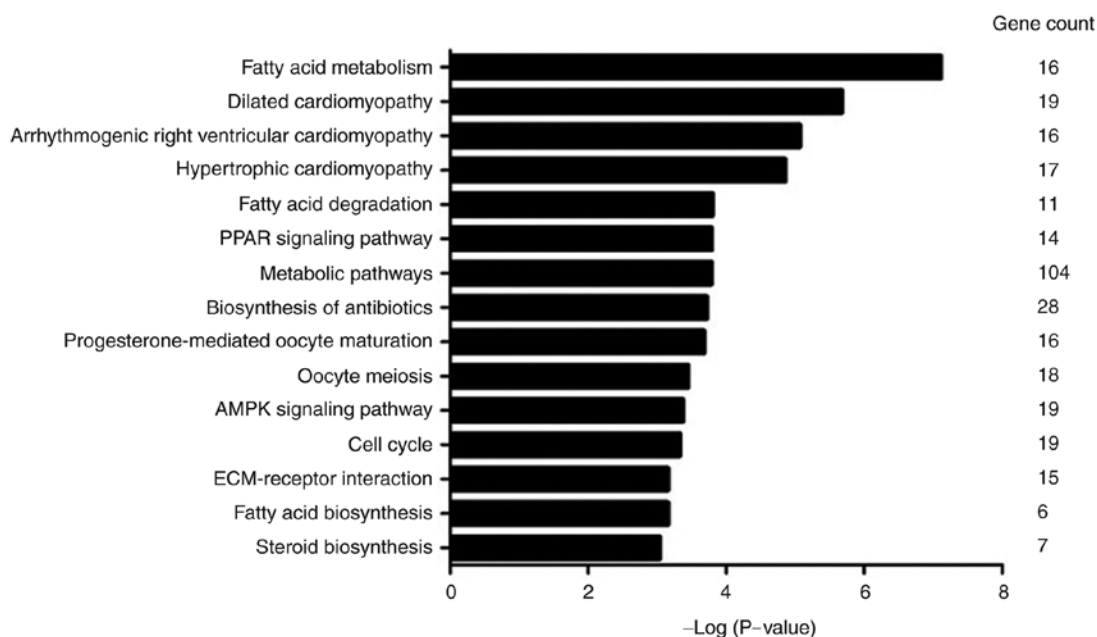


Figure 4. The top 15 significantly enriched pathways associated with the differentially expressed circRNA parental genes according to KEGG analysis. circRNAs, circular RNAs; KEGG, Kyoto Encyclopedia of Genes and Genomes.

hsa_circ_0136134, hsa_circ_0067409, hsa-circRNA9227-1, hsa_circ_0060971, hsa-circRNA9333-2, hsa_circ_0052586, and hsa-circRNA2910-9 potentially interact with 1, 1, 1, 1, 2, 3, and 5 MERs, respectively. The interaction between circRNAs and miRNAs requires further study.

Discussion

Adipocytes are traditionally classified into white, brown, and beige adipocytes (18,19). White adipocytes are involved mainly in energy storage and can trans-differentiate into beige adipocytes and de-differentiate into preadipocyte-like precursors (20-22), while brown and beige adipocytes are involved in adaptive thermogenesis (23). Removing visceral fat (white adipose tissue) (24,25) or increasing the activity or number of beige adipocytes can reverse or reduce metabolic dysfunction, including insulin resistance and obesity (20,26). In the present study, the expression profiles of circRNAs between HPA-v and visceral adipocytes were compared, which were produced

by HPA-v differentiation, to reveal the potential molecular mechanisms of visceral fat accumulation and provide clues for the treatment of visceral obesity.

CircRNAs participate in numerous physiological and pathological processes (13,15,16). However, it is not clear whether circRNAs are associated with adipogenesis and lipid metabolism. Li *et al* reported that circRNAs have different expression profiles in the subcutaneous adipose tissues of the Laiwu pig and Large White pig, which implies that circRNAs participate in subcutaneous adipose deposition (27). In this study, the circRNA expression profiles in HPA-v and adipocytes were first analyzed by microarray analysis, which identified 4,080 circRNAs differently expressed circRNAs in HPA-v and adipocytes, suggesting that HPA-v and adipocytes have different circRNA expression patterns, and that these circRNAs may be associated with visceral adipocyte hyperplasia.

Some circRNAs regulate the expression of their parental gene (e.g., ci-ankrds regulate the ankyrin repeat domain) (28),

sometimes by affecting the alternative splicing of the parental gene (9,29,30). The parental genes of hsa_circ_0136134 and hsa_circ_0017650 are lipoprotein lipase (*LPL*) and inter-alpha-trypsin inhibitor heavy chain 5 (*ITIH5*), respectively. *LPL*, a key enzyme in adipose tissue triglyceride metabolism, is an adipocyte differentiation marker and upregulated during preadipocytes differentiation (31,32). *ITIH5* is a secreted protein, and the *ITIH5* expression in adipose tissue is increased in obesity and reduced after diet-induced weight loss, but the role of *ITIH5* in preadipocyte differentiation has not been reported (33). Thus, hsa_circ_0136134 and hsa_circ_0017650 may influence HPA- α differentiation by regulating the expression of their parental genes. Further studies are required to confirm the regulatory relationship between circRNAs and their parental genes.

Visceral adipocyte hyperplasia is a complex process that involves multiple intracellular signaling pathways. In the present study, the signaling pathways related to fatty acids, which are the substrates of triglyceride synthesis (34), such as 'fatty acid metabolism', 'fatty acid degradation', and 'fatty acid biosynthesis' were enriched. This indicated that circRNAs influence the expression of genes associated with fatty acid metabolism to regulate the accumulation of triglycerides. The 'PPAR signaling pathway', 'AMPK signaling pathway', 'Metabolic pathways', and 'Cell cycle' serve important roles in preadipocyte differentiation, fatty acid oxidation, fatty acid transport, fatty acid synthesis, lipolysis, gluconeogenesis, glycolysis, and cell growth, and may induce the expression of genes related to preadipocyte differentiation or alter the activities of enzymes related to lipid metabolism, contributing to lipid storage. The circRNAs related to these pathways may play critical roles in visceral adipocyte hyperplasia.

CircRNAs can recruit miRNAs to regulate target gene expression (11), and most circRNAs have more than one miRNA binding site; for example, ciRS-7 contains over 60 target sites for miR-7 and can function as a miR-7 sponge and influence miR-7 target gene expression (11). In the present study, it was revealed that the top 10 up- and downregulated circRNAs had many potential miRNA binding sites; for example, hsa-circRNA9227-1, which was upregulated in visceral adipocytes (Table I), contained at least two target sites for hsa-miR-665 (Table II). Previous studies revealed that hsa-miR-665 is downregulated during adipocyte differentiation of human mesenchymal stem cells, and Seipin, which promotes adipocyte differentiation (35), is a potential target gene of miR-665 (36). These results indicated that hsa-circRNA9227-1 was involved in regulating adipogenesis by recruiting hsa-miR-665. However, more research is required to elucidate the function of circRNAs as miRNA sponges in visceral lipid deposition.

The present study assessed the circRNA expression profiles in human visceral preadipocytes and adipocytes. The markedly different circRNA expression profiles between the two cell types reflect the close association between circRNAs and adipogenesis. Further research is required to clarify the function of circRNAs in visceral preadipocyte differentiation and lipid deposition to develop novel therapeutics for obesity.

Acknowledgements

Not applicable.

Funding

The present study was supported by grants from The National Natural Science Foundation of China (grant nos. 81502803 and 31801196), The Natural Science Research Program of Jiangsu Province (grant no. 15KJB330005), and The Shenzhen Science and Technology Innovation Committee (grant no. JCYJ2018030712).

Availability of data and materials

The datasets used/or analyzed during the present study are available from the corresponding author on reasonable request.

Authors' contributions

FD and GX conceived and designed the experiments; WS performed the experiments and drafted the manuscript; and WS, XS, SY and WC performed the data analysis.

Ethics approval and consent to participate

Not applicable.

Patient consent for publication

Not applicable.

Competing interests

The authors declare that they have no competing interests.

References

1. Cefalu WT, Wang ZQ, Werbel S, Bell-Farrow A, Crouse JR III, Hinson WH, Terry JG and Anderson R: Contribution of visceral fat mass to the insulin resistance of aging. *Metabolism* 44: 954-959, 1995.
2. Fujimoto WY, Bergstrom RW, Boyko EJ, Chen KW, Leonetti DL, Newell-Morris L, Shofer JB and Wahl PW: Visceral adiposity and incident coronary heart disease in Japanese-American men. The 10-year follow-up results of the Seattle Japanese-American Community Diabetes Study. *Diabetes Care* 22: 1808-1812, 1999.
3. Sakaguchi M, Fujisaka S, Cai W, Winnay JN, Konishi M, O'Neill BT, Li M, García-Martín R, Takahashi H, Hu J, *et al*: Adipocyte dynamics and reversible metabolic syndrome in mice with an inducible adipocyte-specific deletion of the insulin receptor. *Cell Metab* 25: 448-462, 2017.
4. Silva HM, Bafica A, Rodrigues-Luiz GF, Chi J, Santos PDA, Reis BS, Hoytema van Konijnenburg DP, Crane A, Arifa RDN, Martin P, *et al*: Vasculature-associated fat macrophages readily adapt to inflammatory and metabolic challenges. *J Exp Med* 216: 786-806, 2019.
5. Avram MM, Avram AS and James WD: Subcutaneous fat in normal and diseased states 3. Adipogenesis: From stem cell to fat cell. *J Am Acad Dermatol* 56: 472-492, 2007.
6. Fajas L: Adipogenesis: A cross-talk between cell proliferation and cell differentiation. *Ann Med* 35: 79-85, 2003.
7. Hentze MW and Preiss T: Circular RNAs: Splicing's enigma variations. *EMBO J* 32: 923-925, 2013.
8. Memczak S, Jens M, Elefsinioti A, Torti F, Krueger J, Rybak A, Maier L, Mackowiak SD, Gregersen LH, Munschauer M, *et al*: Circular RNAs are a large class of animal RNAs with regulatory potency. *Nature* 495: 333-338, 2013.
9. Zhang XO, Wang HB, Zhang Y, Lu X, Chen LL and Yang L: Complementary sequence-mediated exon circularization. *Cell* 159: 134-147, 2014.

10. Li Z, Huang C, Bao C, Chen L, Lin M, Wang X, Zhong G, Yu B, Hu W, Dai L, *et al*: Exon-intron circular RNAs regulate transcription in the nucleus. *Nat Struct Mol Biol* 22: 256-264, 2015.
11. Hansen TB, Jensen TI, Clausen BH, Bramsen JB, Finsen B, Damgaard CK and Kjems J: Natural RNA circles function as efficient microRNA sponges. *Nature* 495: 384-388, 2013.
12. Han D, Li J, Wang H, Su X, Hou J, Gu Y, Qian C, Lin Y, Liu X, Huang M, *et al*: Circular RNA circMTO1 acts as the sponge of microRNA-9 to suppress hepatocellular carcinoma progression. *Hepatology* 66: 1151-1164, 2017.
13. Munschauer M, Nguyen CT, Sirokman K, Hartigan CR, Hogstrom L, Engreitz JM, Ulirsch JC, Fulco CP, Subramanian V, Chen J, *et al*: The NORAD lncRNA assembles a topoisomerase complex critical for genome stability. *Nature* 561: 132-136, 2018.
14. Zhao J, Li L, Wang Q, Han H, Zhan Q and Xu M: CircRNA expression profile in early-stage lung adenocarcinoma patients. *Cell Physiol Biochem* 44: 2138-2146, 2017.
15. Legnini I, Di Timoteo G, Rossi F, Morlando M, Briganti F, Sthandier O, Fatica A, Santini T, Andronache A, Wade M, *et al*: Circ-ZNF609 is a circular RNA that can be translated and functions in myogenesis. *Mol Cell* 66: 22-37 e9, 2017.
16. Yang Y, Gao X, Zhang M, Yan S, Sun C, Xiao F, Huang N, Yang X, Zhao K, Zhou H, *et al*: Novel Role of FBXW7 Circular RNA in Repressing Glioma Tumorigenesis. *J Natl Cancer Inst* 110, 2018.
17. Livak KJ and Schmittgen TD: Analysis of relative gene expression data using real-time quantitative PCR and the 2(-Delta Delta C(T)) method. *Methods* 25: 402-408, 2001.
18. Chaurasia B, Kaddai VA, Lancaster GI, Henstridge DC, Sriram S, Galam DL, Gopalan V, Prakash KN, Velan SS, Bulchand S, *et al*: Adipocyte ceramides regulate subcutaneous adipose browning, inflammation, and metabolism. *Cell Metab* 24: 820-834, 2016.
19. Roh HC, Tsai LTY, Shao M, Tenen D, Shen Y, Kumari M, Lyubetskaya A, Jacobs C, Dawes B, Gupta RK and Rosen ED: Warming induces significant reprogramming of Beige, but not brown, adipocyte cellular identity. *Cell Metab* 27: 1121-1137.e5, 2018.
20. Shao M, Ishibashi J, Kusminski CM, Wang QA, Hepler C, Vishvanath L, MacPherson KA, Spurgin SB, Sun K, Holland WL, *et al*: Zfp423 maintains white adipocyte identity through suppression of the beige cell thermogenic gene program. *Cell Metab* 23: 1167-1184, 2016.
21. Wang QA, Song A, Chen W, Schwalie PC, Zhang F, Vishvanath L, Jiang L, Ye R, Shao M, Tao C, *et al*: Reversible de-differentiation of mature white adipocytes into preadipocyte-like precursors during lactation. *Cell Metab* 28: 282-288.e3, 2018.
22. Bi P, Yue F, Karki A, Castro B, Wirbisky SE, Wang C, Durkes A, Elzey BD, Andrisani OM, Bidwell CA, *et al*: Notch activation drives adipocyte dedifferentiation and tumorigenic transformation in mice. *J Exp Med* 213: 2019-2037, 2016.
23. Wang W, Ishibashi J, Trefely S, Shao M, Cowan AJ, Sakers A, Lim HW, O'Connor S, Doan MT, Cohen P, *et al*: A PRDM16-driven metabolic signal from adipocytes regulates precursor cell fate. *Cell Metab* 30: 174-189.e5, 2019.
24. Gabrieli I, Ma XH, Yang XM, Atzmon G, Rajala MW, Berg AH, Scherer P, Rossetti L and Barzilai N: Removal of visceral fat prevents insulin resistance and glucose intolerance of aging: An adipokine-mediated process? *Diabetes* 51: 2951-2958, 2002.
25. Barzilai N, She L, Liu BQ, Vuguin P, Cohen P, Wang J and Rossetti L: Surgical removal of visceral fat reverses hepatic insulin resistance. *Diabetes* 48: 94-98, 1999.
26. Seki T, Hosaka K, Fischer C, Lim S, Andersson P, Abe M, Iwamoto H, Gao Y, Wang X, Fong GH and Cao Y: Ablation of endothelial VEGFR1 improves metabolic dysfunction by inducing adipose tissue browning. *J Exp Med* 215: 611-626, 2018.
27. Li A, Huang W, Zhang X, Xie L and Miao X: Identification and characterization of CircRNAs of two pig breeds as a new biomarker in metabolism-related diseases. *Cell Physiol Biochem* 47: 2458-2470, 2018.
28. Zhang Y, Zhang XO, Chen T, Xiang JF, Yin QF, Xing YH, Zhu S, Yang L and Chen LL: Circular intronic long noncoding RNAs. *Mol Cell* 51: 792-806, 2013.
29. Ashwal-Fluss R, Meyer M, Pamudurti NR, Ivanov A, Bartok O, Hanan M, Evantal N, Memczak S, Rajewsky N and Kadener S: circRNA biogenesis competes with pre-mRNA splicing. *Mol Cell* 56: 55-66, 2014.
30. Kelly S, Greenman C, Cook PR and Papantonis A: Exon skipping is correlated with exon circularization. *J Mol Biol* 427: 2414-2417, 2015.
31. Gong H, Ni Y, Guo X, Fei L, Pan X, Guo M and Chen R: Resistin promotes 3T3-L1 preadipocyte differentiation. *Eur J Endocrinol* 150: 885-892, 2004.
32. Ding ST, McNeel RL and Mersmann HJ: Expression of porcine adipocyte transcripts: Tissue distribution and differentiation in vitro and in vivo. *Comp Biochem Physiol B Biochem Mol Biol* 123: 307-318, 1999.
33. Anveden A, Sjöholm K, Jacobson P, Palsdottir V, Walley AJ, Froguel P, Al-Daghri N, McTernan PG, Mejhert N, Arner P, *et al*: ITIH-5 expression in human adipose tissue is increased in obesity. *Obesity (Silver Spring)* 20: 708-714, 2012.
34. Beale EG, Harvey BJ and Forest C: PCK1 and PCK2 as candidate diabetes and obesity genes. *Cell Biochem Biophys* 48: 89-95, 2007.
35. Bi J, Wang W, Liu Z, Huang X, Jiang Q, Liu G, Wang Y and Huang X: Seipin promotes adipose tissue fat storage through the ER Ca²⁺-ATPase SERCA. *Cell Metab* 19: 861-871, 2014.
36. Yi X, Liu J, Wu P, Gong Y, Xu X and Li W: The key microRNA on lipid droplet formation during adipogenesis from human mesenchymal stem cells. *J Cell Physiol* 235: 328-338, 2020.



This work is licensed under a Creative Commons Attribution-NonCommercial-NoDerivatives 4.0 International (CC BY-NC-ND 4.0) License.